Energy transfer mechanism in Er^{3+} doped fluoride glass sensitized by Tm^{3+} or Ho^{3+} for 2.7-μm emission

Feifei Huang (黄飞飞)[1,2], **Xueqiang Liu (刘雪强)**[1,2], **Weiwei Li (李韦韦)**[1,2],
Lili Hu (胡丽丽)[1], **and Danping Chen (陈丹平)**[1*]

[1]*Key Laboratory of Materials for High Power Laser, Shanghai Institute of Optics and Fine Mechanics,*
Chinese Academy of Sciences, Shanghai 201800, China
[2]*University of Chinese Academy of Sciences, Beijing 100049, China*
[*]Corresponding author: dpchen2008@yahoo.com.cn

Enhanced 2.7 μm emission is obtained in Er^{3+}/Tm^{3+} and Er^{3+}/Ho^{3+} codoped ZBYA glasses. Absorption and emission spectra are tested to characterize the 2.7 μm emission properties of Er^{3+}/Tm^{3+} and Er^{3+}/Ho^{3+} doped ZBYA glasses and a reasonable energy transfer mechanism of 2.7 μm emission between Er^{3+} and Tm^{3+}Ho^{3+}) ion is proposed. Codoping of Tm^{3+} or Ho^{3+} significantly reduces the lifetime of the Er^{3+}: $^4I_{13/2}$ level due to the energy transfer of Er^{3+}:$^4I_{13/2} \rightarrow Tm^{3+}$:$^3F_4$ or Er^{3+}:$^4I_{13/2} \rightarrow Ho^{3+}$: $^5I_7$. Thus, the 2.7 μm emission is strengthened and the 1.5 μm emission is decreased accordingly especially in the Er^{3+}/Tm^{3+} sample. The upconversion effects between the Er^{3+}/Tm^{3+} and Er^{3+}/Ho^{3+} doped ZBYA glasses are different attribute to the different energy transfer efficiencies. Both of the two codoped samples possess nearly equal large emission cross section (16.6×10^{-21} cm^{-2}) around 2.7 μm. The results indicate that this Er^{3+}/Tm^{3+} or Er^{3+}/Ho^{3+} doped ZBYA glass has potential applications in 2.7 μm laser.

OCIS codes: 160.5690, 160.4760, 260.3800.
doi: 10.3788/COL201412.051601.

Recently, interest has been pouring into the mid-infrared spectral region near 3 μm due to the application on medicine, hazardous, chemical detection, coherent lidar, remote atmospheric sensing, and pollution monitoring[1−4]. The transition of $^4I_{11/2} \rightarrow ^4I_{13/2}$ of Er^{3+} ion is favorably employed for the laser emission in the region of 2.7 μm. This transition is "self-terminating", that is, the upper level life time is shorter than the lower level one[5,6]. It is well known that there are three ways to improve the Er^{3+}: 2.7 μm emission: 1, using doping media with low phonon energy and high $^4I_{11/2}$ lifetime to compensate the large quantum defect of Er^{3+}: $^4I_{11/2} \rightarrow ^4I_{13/2}$ and to improve the slope efficiency; 2, depressing the upconversion luminescence of Er^{3+} to reduce heat generation; 3, codoping with other ions to enhance the 2.7 μm emission.

Recent reports about Er^{3+}-doped fiber lasers at 2.7 μm have mainly focused on fluoride glasses (ZBLAN) due to their low phonon energy and low optical attenuation at 3 μm in the typical water absorption band[7−11]. In the past decade, Er-doped and Er-Pr-codoped fluoride fiber lasers have been developed for obtaining higher power output. 10-W level output power at 2.78 μm has been demonstrated with a heavily Er-doped ZBLAN fiber laser[9] and a 24-W liquid-cooled CW 3-μm fiber laser with a multimode-core Er-doped ZBLAN fiber has been developed[12]. However, the stability and output power of fluoride fiber lasers are limited by its low damage threshold, fragility, and low thermal-shock resistance of fluoride glass, not to mention its poor moisture resistance and manufacture difficulty[13]. Thus, exploring effective host matrix becomes a challenge to the researchers. Oxide glass is one candidate with easy preparation, good physical and mechanical performance and good chemical durability. There has been attempt pouring into tellurite

glass[14], bismuthate glass[15], and germinate glass[16] at present. New fluoride glass can also be chosen, such as ZBYA glass, which is a new type of Er^{3+}-doped fluoroziconate glass with better thermal stability[17]. ZBYA glass is proposed to be better resistance to water compared to the ZBLAN glass because of loss of Na. To obtain intense 2.7 μm emission, the artificial depletion of the $^4I_{13/2}$ level is required, which can be achieved by suitable codoping of rear-earth ions and utilizing the energy transfer between levels of the respective ions having equal or close energies[14,18,19]. It has been reported that Tm^{3+} ions can deplete the Er^{3+}: $^4I_{13/2}$ level to obtain 2.7 μm emission in GeGaAsS glass using a titanium-sapphire tunable laser as an excitation source, which can be attributed to the energy transfer between the Tm^{3+}: $^3F_4$ and Er^{3+}: $^4I_{13/2}$ levels[20]. As known, the energy gap between the Er^{3+}: $^4I_{13/2}$ and Ho^{3+}: $^5I_7$ levels is as small as that between Er^{3+}: $^4I_{13/2}$ and Tm^{3+}: $^3F_4$ levels. It is expected both $Tm^{3+}$and Ho^{3+} can deplete the Er^{3+}: $^4I_{13/2}$ level to obtain enhanced 2.7 μm emission. Few results have been reported on the 2.7 μm emission in Er^{3+}/Tm^{3+} or Er^{3+}/Ho^{3+} doped ZBYA glass pumped by a common 980 nm laser diode (LD).

In this letter, Er^{3+}/Tm^{3+} and Er^{3+}/Ho^{3+} doped ZBYA glasses are prepared, the 2.7 μm spectroscopic properties have been investigated and the energy transfer mechanism between Er^{3+} and Tm^{3+} (Ho^{3+}) has been discussed. The glasses show potential applications for mid-IR laser media.

The investigated glass has the following molar compositions:

$50ZrF_4$–$33BaF_2$–$17(AlF_3+YF_3)$–$1ErF_3$-X(X=0, $1TmF_3$, $1HoF_3$ singed as E1, E1T1, E1H1, respectively)

All the samples were prepared by using high-purity

ZrF_4, BaF_2, YF_3, AlF_3, ErF_3, TmF_3, and HoF_3 powder. Well-mixed 25 g batches of the samples were placed in platinum crucibles and melted at about 1000 °C for 30 min. Then the melts were poured onto a preheated copper mold and annealed in a furnace around the glass transition temperature. The annealed samples were fabricated and polished to the size of 20×15×1 (mm) for the optical property measurements.

The characteristic temperatures (temperature of glass transition T_g and temperature of onset crystallization peak T_x) of samples were determined using a NetzschSTA449/C differential scanning calorimetry at a heating rate of 10 K/min. The density and refractive index of the samples were measured by the Archimedes method using distilled water as an immersion liquid and the prism minimum deviation method respectively. Furthermore, the absorption spectra were recorded with a Perkin-Elmer Lambda 900 UV/VIS/ NIR spectrophotometer in the range of 390–1600 nm, and the emission spectra were measured with a Triax 320 type spectrometer (Jobin-Yvon Co., France). All the measurements were carried out at room temperature.

The temperature of glass transition T_g and temperature of inset crystallization peak T_x are determined using a NetzschSTA449/C differential scanning calorimetry at a heating rate of 10 K/min. The glass forming ability criterion, $\Delta T(T_x - T_g)$, has been frequently used to measure the glass stability and a large ΔT means strong inhibition of nucleation and crystallization[21,22]. The ΔT of present three samples is calculated about 90 °C±5 °C which is larger than those of ZBLAN glass (82 °C)[23] and ZBLA glass (74 °C)[23]. A larger ΔT also means a wide working range of temperature during fiber drawing. Based on present glasses, it is desirable to achieve a larger working range during fiber drawing. Moreover, it is necessary to possess a high T_g which will minimize the thermal damage when pumped by high power lasers[24]. The T_g of present glasses (330 °C±5 °C) is high than ZBLA glass (316 °C)[23], ZBLAN glass (276 °C)[23], and ZBSA glass (301 °C)[25].

Figure 1 demonstrates the absorption spectra of Er^{3+} singly doped, Er^{3+}/Tm^{3+} and Er^{3+}/Ho^{3+} codoped ZBYA glasses in the wavelength region of 390–1600 nm. The absorption bands of Er^{3+}, Tm^{3+} and Ho^{3+} corresponding to transitions starting from the ground state to higher levels are labeled. Generally, for the E1T1 and E1H1 samples, the shape and peak positions of each transition are very similar to other Er^{3+}, Tm^{3+} and Ho^{3+} doped glasses and there is no shift in the wavelength of the absorption peaks[26,27]. This phenomenon indicates no cluster in the local ligand field and three kinds of ions are homogeneously incorporated into the glassy network. The strong absorption around 980 nm indicates that the present samples can be excited efficiently by a 980 nm LD.

As we know, the content of OH^- in glass is related to the emission efficiency of rare-earth ions, as the residual OH^- groups will participate in the ET (energy transfer) of rare-earth ions and reduce the intensity of emission[28]. The IR transmittance spectra of the prepared glasses, indicating the OH^- content, are shown in the inset of Fig. 1. It can be seen that the maximum transmittance
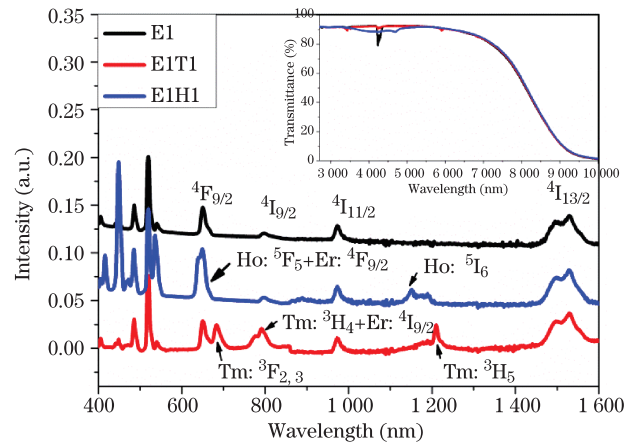

Fig. 1. Absorption spectra of prepared samples and the inset is the transmittance spectra of the samples.

reaches as high as 90% all of the samples. The 10% loss contains the Fresnel reflections, dispersion, and absorption of the glass. The content of OH- groups in the glass can be expressed by the absorption coefficient of the OH^- vibration band at 3 μm which can be given by

$$\alpha_{OH^-} = \ln(T/T_0)/l, \tag{1}$$

where l is the thickness of the sample at 1 mm, and T_0 and T are the transmitted and incident intensities respectively. The calculated absorption coefficients of the samples are 0.056, 0.045, 0.088 cm^{-1} respectively, which is much lower than those of the fluorophosphates glass[29] and tellurite glass[14]. Meanwhile, the litter absorption band about 4500 nm is due to the CO_2 absorption and absorption around 6200 nm is owing to the fundamental of fluoride glass. The good IR transmission property proves that the ZBYA glass is a potential candidate for IR laser materials.

Figure 2(a) shows the fluorescence spectra of the three samples in the region of 1450–1750 nm and inset of Fig. 2(a) shows the fluorescence spectrum of E1T1 glass in the region of 1400–1900 nm and the fluorescence spectrum of E1H1 glass in the region of 1950–2100 nm. Introducing of Tm^{3+} or Ho^{3+} results in a large decrease in the 1550 nm emission intensity, which can attribute to the energy transfer process ET2 ($Er^{3+}:^4I_{13/2} \rightarrow Tm^{3+}:^3F_4$) or ET6 ($Er^{3+}:^4I_{13/2} \rightarrow Ho^{3+}: ^5I_7$) (Fig. 3). The ET6 process has lower efficiency due to the larger gap between $Er^{3+}:^4I_{13/2}$ and $Ho^{3+}: ^5I_7$. It is worth mentioning that there is an emission at ~1.8 μm due to the $Tm^{3+}:^3F_4 \rightarrow ^3H_6$. Since Tm^{3+} has no absorption band matching the 980 nm excitation used for the experiment, there appears to be an energy transfer from Er^{3+} to Tm^{3+}. There is a similar phenomenon in the E1H1 sample.

Emission at 2708 nm due to the $Er^{3+}: ^4I_{11/2} \rightarrow ^4I_{13/2}$ is clearly observed as shown in Fig. 2(b). It is found that their emission shape is very similar, but the intensity increases dramatically especially in the E1T1 sample. As Tm^{3+} or Ho^{3+} is introduced into $Er^{3+}:$ ZBYA glass, there are several other additional energy transfer processes except ET2 and ET6:

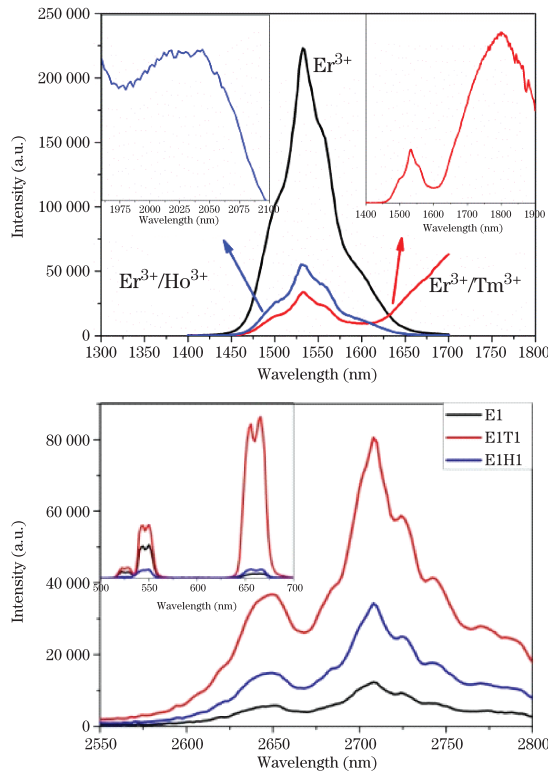ET1: ($Er^{3+}: ^4I_{11/2}+Tm^{3+}: ^3H_6$) $\rightarrow$($Er^{3+}: ^4I_{15/2}+$ $Tm^{3+}: ^3H_5$),
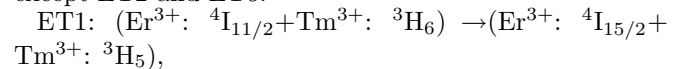
Fig. 2. Diode-pumped (980nm) fluorescence spectra of present samples (a) 1550 and (b) 2708μm emission. Inset of (a) is the fluorescence spectra of ET glass around 1.8 μm and EH glass around 2 μm. Inset of (b) is the fluorescence spectra from 400–700 nm.

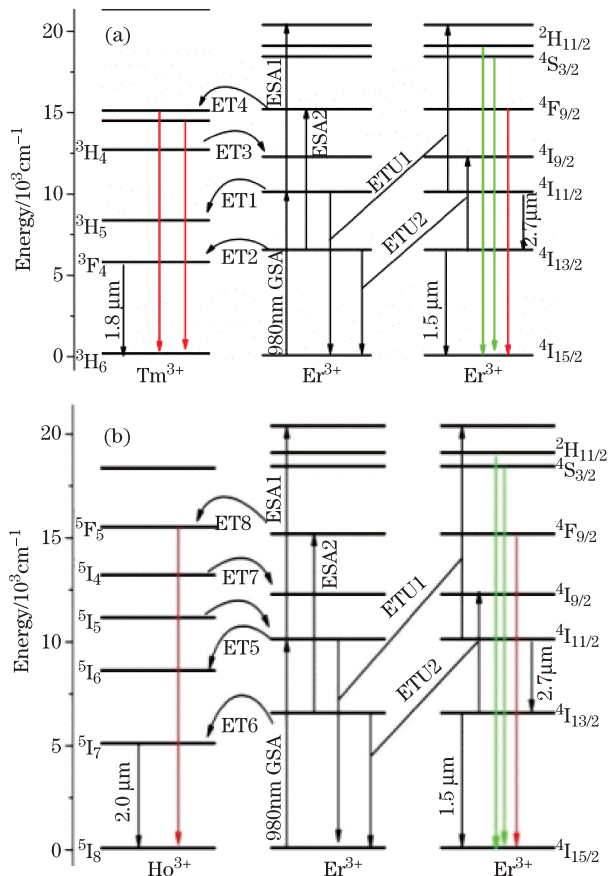Fig. 3. Energy level (a) Er^{3+} and Tm^{3+} (b) Er^{3+} and Ho^{3+}.

ET5: (Er^{3+}:$^4I_{11/2}$+Ho^{3+}: $^5I_8$) →(Er^{3+}: $^4I_{15/2}$+ Ho^{3+}: $^5I_6$),

ET3: (Er^{3+}: $^4I_{15/2}$ + Tm^{3+}: $^3H_4$) →(Er^{3+}: $^4I_{9/2}$ + Tm^{3+}: $^3H_6$),

ET7: (Er^{3+}: $^4I_{15/2}$ + Ho^{3+}: $^5I_4$) →(Er^{3+}: $^4I_{9/2}$ + Ho^{3+}: $^5I_8$),

(Er^{3+}: $^4I_{15/2}$ + Ho^{3+}: $^5I_5$) →(Er^{3+}: $^4I_{11/2}$ + Ho^{3+}: $^5I_8$),

ET4: (Er^{3+}: $^4F_{9/2}$+ Tm^{3+}: $^3H_6$) →(Er^{3+}: $^4I_{15/2}$ + Tm^{3+}: $^3F_2/^3F_3$),

ET8: (Er^{3+}: $^4F_{9/2}$ + Ho^{3+}: $^5I_8$) →(Er^{3+}: $^4I_{15/2}$ + Ho^{3+}: $^5F_5$).

The enhanced 2.7 μm emission can be explained by the energy transfer processes by two sides. The ET2 or ET6 depopulating the Er^{3+}: $^4I_{13/2}$ is more efficient than the ET1 or ET5 depopulating the Er^{3+}: $^4I_{11/2}$. On the other hand, the existence of ET3 or ET7 process increases the ions on the Er^{3+}: $^4I_{11/2}$ level. In addition, according to the Fuchtbauer-Ladenburg theory[30−32], the 2.7 μm emission cross section in the E1T1 and E1H1 samples are 16.64×10^{-21} and 16.63×10^{-21} cm^{-2}, respectively. The values are much higher than the reported ones of 5.4×10^{-21} cm^{-2} in Er^{3+} doped ZBLAN glass[33] and 6.02×10^{-21} cm^{-2} in Er^{3+}/Tm^{3+} /Ho^{3+} triply doped FP glass[26].

The inset of Fig. 2(b) shows the upconversion luminescence of the samples. Green upconversion emissions centered around 525 and 545 nm occur in Er^{3+} singly doped sample because of the $^2H_{11/2}$ →$^4I_{15/2}$ and $^4S_{3/2}$ →$^4I_{15/2}$ transitions from GSA and GSA1. The enhanced green emission in the E1T1 sample can be explained by the increased ions on the $^4I_{11/2}$ duo to the ET3 process. While, the situation in the E1H1 sample is different, the ET5 process decreases the ions on the $^4I_{11/2}$ more efficiently than the ET7 process, the combined effect causes the decreased intensity of green emission. The enhanced red emission both in the ET and in EH sample mainly attribute to the ET4 and ET8 process.

The 1.55 μm emission happens owing to the Er^{3+}:$^4I_{13/2}$ →$^4I_{15/2}$ transition. It has mentioned the 1.55 μm emission drops due to the ET2 or ET6 process while the 2.7 μm emission increases because of the ET2 (ET6) is much more efficient than the ET1 (ET5) process. The ET efficiency has been estimated from the lifetime values by the following equation[34]:

$$\eta_t = 1 - \frac{\tau_{Er/Tm(Ho)}}{\tau_{Er}}, \qquad (2)$$

where $\tau_{Er/Tm(Ho)}$ and τ_{Er} are the Er^{3+} lifetimes monitored at 1.5 μm with and without Tm^{3+} (Ho^{3+}) ions, respectively. The value of η_t from ET2 process is up to 55% from Tm^{3+}/Er^{3+}-codoped ZBYA glass as shown in Fig. 4, while the value in the EH sample is little lower (45%). It is demonstrated that Tm^{3+} or Ho^{3+}can efficiently quench the lower laser level of Er^{3+} and enhance the emission of 2.7 μm.

In conclusion, Er^{3+}/Tm^{3+} and Er^{3+}/Ho^{3+} doped ZBYA glasses with good thermal stability are prepared. An extensive transmission spectra and absence of strong OH$^-$ absorption at 3 μm guarantee the observation of intense 2.7 μm emission. With the introducing of Tm^{3+}
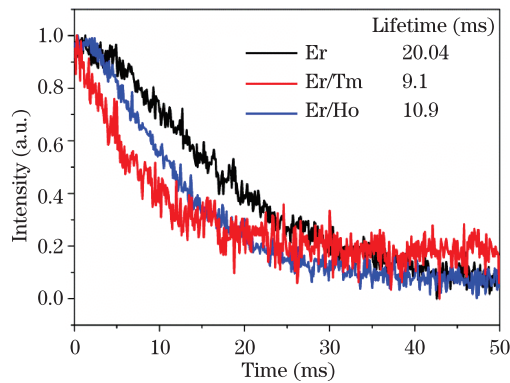
Fig. 4. Fluorescence decay curves of E1, E1H1 and E1T1 glasses for the ${}^4I_{13/2}$ mainfold.

or Ho^{3+} into the ZBYA system, the enhanced 2.7 μm emission and decreased 1.5 μm emission are obtained. The energy transfer processes between Er^{3+} and Tm^{3+} (Ho^{3+}) are analyzed and it is found that the upconversion effect between the two codoped samples is different. Both of the two codoped samples possess nearly equal large emission cross section (16.6×10^{-21} cm^{-2}) around 2.7 μm. The present results suggest that the Er^{3+}/Tm^{3+} or Er^{3+}/Ho^{3+} doped ZBYA glasses can be considered as a promising material for a 2.7 μm laser.

References

1. S. Yang, X. Wang, and H. Guo, Opt. Express **19,** 26529 (2011).
2. S. D. Jackson, T. A. King, and M. Pollnau, Opt. Lett. **24,** 1133 (1999).
3. A. S. de Camargo, E. R. Botoa, D. Garcia, and J. A. Eiras, Appl. Phys. Lett. **86,** 241112 (2005).
4. C. Guo, D. Shen, J. Long, and F. Wang, Chin. Opt. Lett. **10,** 091406 (2012).
5. X. Li, X. Liu, L. Zhang, L. Hu, and J. Zhang, Chin. Opt. Lett. **11,** 121601 (2013).
6. G. Zhao, Y. Tian, H. Fan, J. Zhang, and L. Hu, Chin. Opt. Lett. **10,** 091601 (2012).
7. T. Sandrock, A. Diening, and G. Huber, Opt. Lett. **24,** 382 (1999).
8. Y. Tian, R. Xu, L. Hu, and J. Zhang, Opt. Mater. **34,** 308 (2011).
9. X. Zhu and R. Jain, Opt. Lett. **32,** 26 (2006).
10. X. Zhu and R. Jain, Opt. Lett. **33,** 1578 (2008).
11. Y. Tian, R. Xu, L. Hu, and J. Zhang, J. Am. Ceramic. Soc. **94,** 2289 (2011).
12. S. Tokita, M. Murakami, S. Shimizu, M. Hashida, and S. Salabe, Opt. Lett. **34,** 3062 (2009)..
13. X. Zhu and N. Peyghambarian, Adv. OptoElectron. **2010,** 501956 (2010).
14. S. Guan, Y. Tian, Y. Guo, L. Hu, and J. Zhang, Chin. Opt. Lett. **10,** 071603 (2012).
15. Y. Guo, M. Li, L. Hu, and J. Zhang, Opt. Lett. **37,** 268 (2012).
16. R. Xu, Y. Tian, L, Hu, and J. Zhang, J. Appl. Phys. **111,** 033524 (2012).
17. F. Huang, Y. Guo, and Y. Ma, Appl. Opt. **52,** 1399 (2013).
18. Z. Zhu, J. Li, Z. You, Y. Wang, S. Lv, E. Ma, J. Xu, H. Wang, and C. Tu, Opt. Lett. **37,** 4838 (2012).
19. Y. Tian, R. Xu, L. Hu, and J. Zhang, J. Quant. Spectrosc. Rad. Trans. **113,** 87 (2012).
20. Y. Choi, K. Kim, B. J. Lee, Y. B. Shin, Y. S. Kim, and J. Heo, J. Non-Cryst. Solids **278,**137 (2000).
21. S. Xu, Z. Yang, and Z. Jiang, J. Alloy Comp. **361,** 313 (2003).
22. D. Jia, Y. Chen, W. Chen, L. Hu, and G. Boulon, Chin. Opt. Lett. **10,** 071602 (2012).
23. R. Lebullenger, S. Benjaballah, C. LeDeti, and M. Pollutain, J. Non-Cryst. Solids **161,** 217 (1993).
24. R. Xu, Y. Tian, L. Hu, and J. Zhang, Opt. Lett. **36,** 1173 (2011).
25. M. Pollnau, E. Heumann, and G. Huber, Appl.Phys. A **54,** 404 (1992).
26. Y. Tian, R. Xu, L. Hu, and J. Zhang, Opt. Lett. **36,** 3218 (2011).
27. L. Zhang, Z. Yang, Y. Tian, J. Zhang, and L. Hu, J. Appl. Phys. **110,** 093106 (2011)..
28. A. Lin, A. Ryasnyanskity, and J. Toulouse, Opt. Lett. **36,** 740 (2011).
29. Y. Tian, R. Xu, L. Hu, and J. Zhang, J. Appl. Phys. **108,** 083504 (2010).
30. S. Payne, L. Chase, L. Smith, W. Kway, and W. Krupke, IEEE J. Quant. Electron. **28,** 2619 (1992).
31. V. K. Tikhomirov, J. Mendez-Ramos, V. D. Rodriguez, D. Furniss, and A. B. Sedden, Opt. Mater. **28,** 1143 (2006).
32. X. Wang, L. Hu, K. Li, Y. Tian, and S. Fan, Chin. Opt. Lett. **10,** 101601 (2012).
33. H. Lin, D. Chen, and Y. Yu, Opt. Lett. **36,** 815 (2011).
34. W. T. Carnall, P. R. Fields, and K. Rajnak, J. Chem. Phys. **49,** 4412 (1968).